Electron Kinetics Induced by Ultrafast Photoexcitation of Warm Dense Matter in a 30-nm-Thick Foil

Z. Chen, Y. Y. Tsui, M. Z. Mo, R. Fedosejevs, T. Ozaki, V. Recoules, P. A. Sterne, and A. Ng

Phys. Rev. Lett. **127**, 097403 — Published 27 August 2021

DOI: 10.1103/PhysRevLett.127.097403

Electron kinetics induced by ultrafast photoexcitation of warm dense matter in a thin gold foil

Z. Chen[†],[1,*] Y.Y. Tsui,[1] M.Z. Mo,[1,†] R. Fedosejevs,[1] T. Ozaki,[2] V. Recoules,[3] P.A. Sterne,[4] and A. Ng[5,‡]

[1]*Department of Electrical and Computer Engineering, University of Alberta, Edmonton, Alberta, Canada*
[2]*INRS-EMT, University of Quebec, Varennes, Quebec, Canada*
[3]*CEA, DAM, DIF, 91297 Arpajon Cedex, France*
[4]*Lawerence Livermore National Laboratory, Livermore, CA, U.S.A.*
[5]*Department of Physics and Astronomy, University of British Colombia, Vancouver, B.C, Canada*

We report on the study of electron kinetics induced by intense, fs-laser excitation of electrons in the $5d$ band of Au. Changes in the electron system are observed from the temporal evolution of ac conductivity and conduction electron density. The results reveal an increase of electron thermalization time with excitation energy density, in contrary to the Fermi-liquid behavior of the decrease of thermalization time associated with the heating of conduction electrons. This is attributed to the severe mitigation of photo-excitation by Auger decay. The study also uncovers the shortening of $5d$ hole lifetime with the increase of photo-excitation rates. These unique findings provide valuable insights for understanding electron kinetics under extreme non-equilibrium conditions.

PACS numbers: 52.50.Jm, 52.27.Gr, 71.15.-m, 72.80.-r

In non-equilibrium Warm Dense Matter research, experiments have long been focused on states with unequal electron and ion temperatures. These include studies of electrical conductivity and dielectric function [1–4], electron-ion coupling [5–14] and lattice stability [7, 8, 14, 15]. However, little is known about the states with non-Fermi-Dirac electron energy distribution and in particular the effects of electron kinetics under such non-equilibrium conditions. The missing information is not only of fundamental interest, it is also becoming a vital focus in the rapidly expanding investigations of Warm Dense Matter produced by ultrafast heating of solids using high-intensity lasers, FELs and laser-generated particle beams. Common among these states are their strongly out-of-equilibrium electron systems. As yet, investigations have been concerned with photo-excitation of conduction electrons at very low laser fluences. A seminal study is the photoemission spectroscopy measurement of the temporal evolution of electron energy distribution in Au heated by 1.84eV, 180fs laser pulses [16]. The results show that thermalization time is reduced from 1300fs to 670fs when the absorbed laser fluence is increased from 120μJ/cm^2 to 300μJ/cm^2. The behavior is modeled with some success using Boltzmann equation calculations in the relaxation time approximation while treating energy transfer from electron to ions with an electron-ion coupling constant of 4×10^{16}W/m^{3}K. The experimental data are in much better agreement with numerical solutions of the Boltzmann equation for the one-particle matrix [17], albeit for an electron-ion coupling constant of 2.7×10^{17}W/m^{3}K. On the other hand, later measurements of transient reflectivity and transmissivity in 1.06μm-800nm, 140fs laser heated Au suggest that electron thermalization occurs in ∼500fs, independent of incident laser fluence between 2.5-200μJ/cm^2 [18]. However, this finding also contradicts the results of Boltzmann calculations incorporating the density of states of $5d$ and $6s, p$ electrons that show the decrease in electron thermalization time with absorbed laser fluence between 10 to 650μJ/cm^2 [19]. On the other hand, the new and pressing question is how electron kinetics behaves in the far broader regime of strongly out-of-equilibrium Warm Dense Matter where (a) the excitation energy density readily exceeds 1 eV/atom and (b) the density of photoelectrons readily exceeds 1 electron/atom. It may also be noted that this is a distinctly different regime than photoexcitation of semiconductors where significant advances have been made [20–22].

Here, we report on the study of the effects of electron kinetics during electron thermalizaton in photo-excitation of $5d$ electrons in non-equilibrium warm dense Au. In the experiment a 400nm, 48fs (FWHM) laser pulse is focused at normal incidence to a 100μm-FWHM Gaussian spot on a 30nm-thick, freestanding Au foil in vacuum. The pre-pulse contrast of the 800nm laser beam is 10^{-4} at 0.5ps prior to the peak of the pulse [23]. The corresponding contrast of the 400nm laser beam is estimated to be $\sim10^{-8}$. Laser absorption in the foil is determined directly from simultaneous measurements of the incident, transmitted and reflected laser beams with a spatial resolution of 5μm. This shows that the process remains linear for incident fluences up to 0.55J/cm^2. The measured absorption of 47±4% is in good agreement with the value calculated from the known dielectric function of Au at normal conditions for photon energy of 3.1eV (400nm) where the $5d$-$6sp$ interband contributions dominate [24]. In this study, we have thus limited the maximum incident fluence to 0.53J/cm^2 (with corresponding absorbed energy density of 4.3MJ/kg) where laser absorption leads to single-photon excitation of $5d$ electrons.

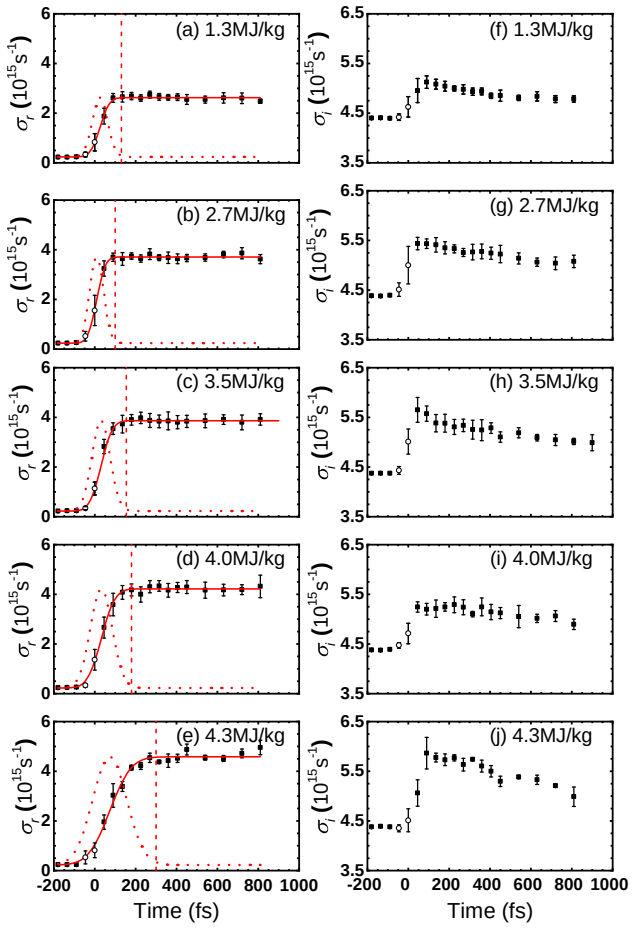

FIG. 1. The temporal evolution of σ_r and σ_i at 800nm. Time zero corresponds to the time of peak pump laser intensity. The data points at time zero and -45fs are denoted by open circles as a reminder that at these early times, energy deposition in the foil may not be uniform. The red line is a cumulative Gaussian function best fitted to data. The red dotted line (in arbitrary unit) shows the underlying Gaussian function. The vertical red dashed line marks the electron thermalization time.

For incident fluences above 0.55J/cm^2, the reduction in laser absorption has been attributed to the effect of inhibited ballistic electron transport [25].

To monitor the effect of electron kinetics, we follow the temporal evolution of the optical properties of the heated foil. An 800nm, 51fs (FWHM) probe laser pulse is used to illuminate at 45^o incidence an ~1mm-diameter spot that is concentric with the pump laser focal spot. The reflectivity R and transmissivity T of the probe are measured from a central 30μm-diameter region of the pump laser spot while an unheated region of the foil is used to provide *in-situ* calibration. Across this 30μm-diameter region, the pump laser fluence varies by $\pm$7% from its mean value. Here, the absorbed fluence Φ_{abs} and the corresponding excitation energy density $\Delta\varepsilon$ ($\Delta\varepsilon$=Φ_{abs}/L and L is foil thickness of 30nm) refer to their mean values. The original R, T data are presented in the Supplemental Materials. As R and T are determined by both the optical properties and the thickness of the heated sample, it is more definitive to examine instead ac conductivity that is an intrinsic physical property of the state. This is obtained from the solution of the Helmholtz equations for the propagation of an electromagnetic wave in a uniform dielectric slab (the heated foil), using R and T as the input parameters [1, 2, 26]. The temporal evolution of the real and imaginary parts of ac conductivity (σ_r and σ_i) is presented in Fig. 1. Laser excitation causes σ_r to increase until it reaches quasi-steady-state maximum. The onset of the quasi-steady-state is delayed more and more with increasing $\Delta\varepsilon$. In contrast, σ_i is found to increase to a local maximum, followed by a slow decrease. The time it takes to reach this local maximum appears independent of $\Delta\varepsilon$. These different temporal behaviors can be attributed to the origin of the two quantities. As described by the Kubo-Greenwood formula, σ_r sums the contributions from all allowed transitions at a specific probe photon frequency. With the 1.55eV (800nm) probe, σ_r is effectively sampling the DOS in the conduction band and hence uniquely sensitive to the free electron density. On the other hand, σ_i includes contributions from σ_r at all frequencies as defined by the Kramers-Kronig relation. It is thus sensitive to the entire electron distribution in the DOS.

With its direct link to the DOS of the $6sp$ band, σ_r is of particular interest. In the absence of theoretical predictions, $\sigma_r(t)$ is fitted with a cumulative Gaussian function $F(t) = \int_{-\infty}^{t} f(t)dt$, where $f(t)$ is the underlying Gaussian function given by $f(t)$=exp($-t^2/\tau^2$) and τ is its 1/e time constant, as illustrated in Fig. 1. In this representation, $f(t)$ corresponds to the temporal rate of change of σ_r resulting from the competing electron kinetics processes that drive σ_r towards a quasi-steady-state value. For practical reasons, the onset of the quasi-steady-state is taken to occur at $t = 2\tau$ where $F(t)$ reaches 99.7% of it maximum value, as indicated by the vertical red dashed lines in Fig. 1. To understand the physical meaning of the quasi-steady-state, Fig. 2(a) shows the comparison of the quasi-steady-state value of σ_r with that measured at the time when the electron subsystem is thermalized [2]. The good agreement indicates that electron thermalization is achieved in the quasi-steady-state. Accordingly, the time to reach the quasi-steady-state of σ_r is also the electron thermalization time τ_{th}. This finding is presented in Fig. 2(b). It reveals the increase of τ_{th} with excitation energy density above 2.7MJ/kg. This contradicts the familiar Fermi-liquid behavior of the decrease of τ_{th} with energy density seen in the heating of conduction electrons [16–19]. The new phenomenon is evidently linked to the excitation of $5d$ electrons in Au. It may be noted that the apparently constant τ_{th} below 2.7MJ/kg reflects the temporal resolution limit of our measurement.

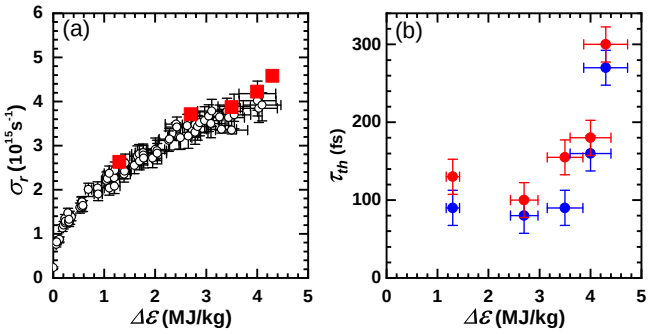

FIG. 2. (a) σ_r as a function of excitation energy density $\Delta\epsilon$. The red squares are the new data and the black circles are data taken from [2]. (b) τ_{th} as a function $\Delta\epsilon$. The red and blue circles are results derived from $\sigma_r(t)$ and $n_e(t)$ respectively. The error bars for τ_{th} correspond to uncertainties resulting from the discrete time steps.

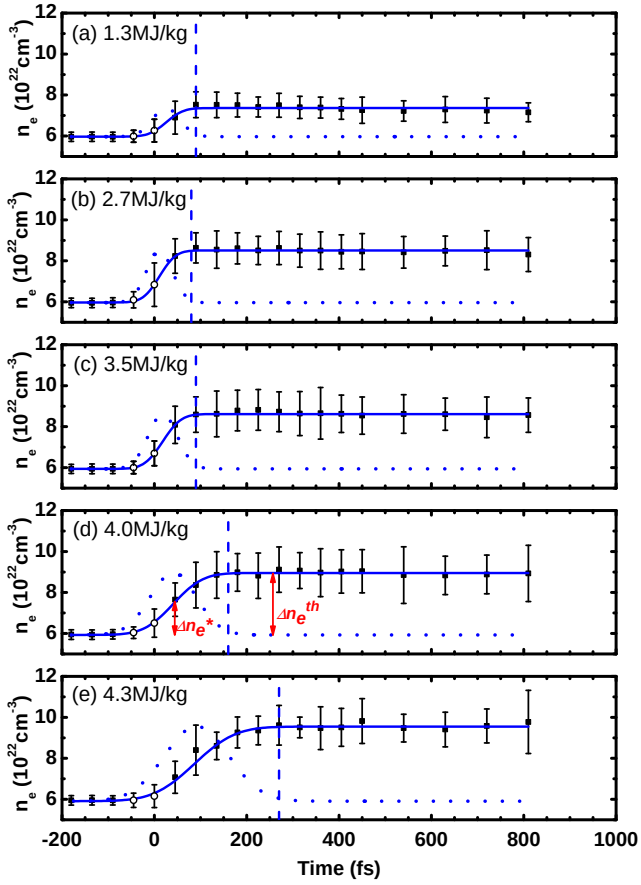

FIG. 3. Temporal evolutions of n_e. Time zero corresponds to the time of peak pump laser intensity. The data points at time zero and -45fs are denoted by open circles as a reminder that at these early times, energy deposition in the foil may not be uniform. The blue line is a cumulative Gaussian function best fitted to data. The blue dotted line (in arbitrary unit) shows the underlying Gaussian function. The vertical blue dashed line marks the electron thermalization time.

To shed light on the effect of electron kinetics prior to thermalization, we turn our attention to the conduction electron density n_e that can be compared directly with results of electron kinetics calculations. To determine n_e, we note that Drude behavior of the imaginary part of the dielectric function ε_i for photon energies below 1.9eV has been observed in fs-laser heated Au in both the thermalized states with energy density up to 4.7MJ/kg and the states prior to thermalization with energy density of 2.9MJ/kg [4]. This indicates that the dielectric function is dominated by intraband contributions of $6sp$ electrons, while the $5d$ intraband contributions and $5d$-$6sp$ interband contributions play a minor role. The finding leads to the derivation of n_e using a Drude-model interpretation of the dielectric function obtained from the measured ac conductivity [27]. Following the same approach, we have deduced the temporal evolution of n_e as presented in Fig. 3. The similar temporal characteristics of $n_e(t)$ and $\sigma_r(t)$ is the result of the Drude behavior. Hence, a cumulative Gaussian distribution function is also fitted to $n_e(t)$. This yields electron thermalization times similar to those derived from $\sigma_r(t)$ within the uncertainties introduced by the discrete time steps, as shown in Fig. 2(b).

Here, of even greater significance is the increase in electron density Δn_e* at the end of laser excitation at t=45fs (as identified in Fig. 3d), where Δn_e*=(n_e* - n_{e0}), n_e* is the electron density at t=45fs and n_{e0}=5.9×10^{22} cm^{-3} is the initial electron density. The first important finding is Δn_e*$\ll n_{pe}$*, the total density of the photoelectrons produced during the pump laser pulse, as shown in Fig. 4(a). For single-photon absorption, n_{pe}*=$\Delta\varepsilon/(e\cdot h\nu)$ cm^{-3} where e=electron charge and $h\nu$=3.1eV. This reveals that during the pump laser pulse, photo-excitation of the $5d$ electrons is severely mitigated by Auger decay of the $5d$ holes. The impact of this behavior is far reaching. As shown in Fig. 4(b), Auger decay also renders Δn_e* less than Δn_e^{th}, the increase in electron density at thermalization defined by the difference between the quasi-steady-state and the initial electron densities (as marked in Fig. 3d). This means that at the end of photo-excitation, Auger decay causes the density of $6sp$ electrons to fall below that of a thermalized electron system, creating a strongly out-of-equilibrium system. A further discovery is that Δn_e* lags increasingly behind Δn_e^{th} for $\Delta\varepsilon$ above 2.7MJ/kg. This indicates that more intense photo-excitation leads to escalating deviations of the occupation of the $5d$ and $6sp$ bands from equilibrium. The phenomenon is crucial for understanding the subsequent thermalization process.

To quantify the effect of Auger decay, we consider the change in atomic configurations via (i) photo-excitation of $5d^{10}6s+h\nu\rightarrow 5d^9 6s6p$ and (ii) Auger decay of $5d^9 6s6p$ $\rightarrow$ $5d^{10}+e_{Auger}$. The density n_2 of the photo-excited state $5d^9 6s6p$ can be described by the rate equation:

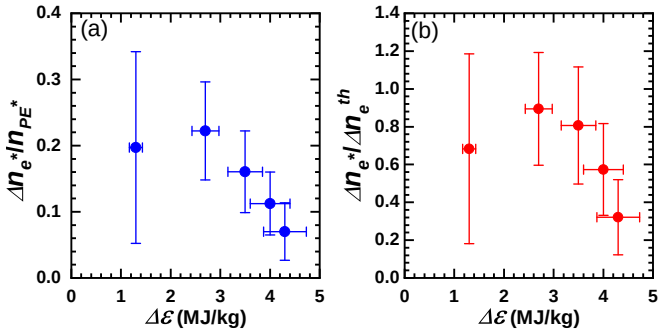

FIG. 4. The dependence of (a) $(\Delta n_e^*/n_{pe}^*)$ and (b) $(\Delta n_e^*/\Delta n_e^{th})$ on excitation energy density $\Delta\varepsilon$.

$$\frac{dn_2(t)}{dt} = \Gamma_{PE}(t) - \gamma_2 n_2(t) \quad (1)$$

where $\Gamma_{PE}(t)=I_{abs}(t)/(d.e.h\nu)cm^{-3}\cdot s^{-1}$ is the rate of increase of n_2 due to single-photon excitation, I_{abs} is the absorbed pump laser intensity in units of W/cm^2, d=sample thickness=$3\times10^{-6}cm$, and the Auger decay rate γ_2 is given by $1/\tau_h$ assuming a constant lifetime τ_h of $5d$ holes. Fig. 5 shows $\Gamma_{PE}(t)$ for $\Delta\varepsilon$ of 4MJ/kg and the corresponding $n_2(t)$ for different values of τ_h. Here, $n_2(t)$ has been convoluted with a 51fs(FWHM) Gaussian instrumental function to facilitate comparison with observations. Since the $5d^9 6s6p$ configuration corresponds to the addition of a photoelectron in the $6sp$ band, Δn_e* is the same as $n_2(t$=45fs). From Fig. 5, it is evident that $n_2(t$=45fs) is strongly dependent on τ_h. We can thus use the values of Δn_e* from Fig. 3 to deduce the corresponding values of τ_h at different excitation energy densities. This yields the first assessment of $5d$ hole lifetime in strongly out-of-equilibrium Warm Dense Matter. Equally significant, the results uncover the shortening of τ_h with the increase of excitation energy density $\Delta\varepsilon$, as shown in Fig. 6. Here, it is important to recognize that $\Delta\varepsilon$ is time-integrated over the total duration (∼90fs) of the pump laser pulse. With τ_h of 10-22fs, it seems more pertinent to quantify the role of laser excitation by the photo-excitation rate and in particular the photo-excitation rate $\Gamma_{PE}(t$=0) at the time of peak pump laser intensity (Fig. 5). Accordingly, we have correlated the shortening of τ_h directly with the increase of $\Gamma_{PE}(t$=0) as presented in Fig. 6. Furthermore, we may note that although our deduced τ_h is consistent with the predicted lifetimes in the range of 10fs-22fs for $5d$ holes with energy of 3.1ev to 2eV below the Fermi energy in Au at normal conditions [28], our values should be considered as upper bounds since the secondary process of collisional excitation of $5d$ electrons has not been included in our rate equation.

With the above findings, we can also construct a physical picture to describe electron kinetics induced by ultrafast photo-excitation of $5d$ electrons in Au. During the pump laser pulse, single-photon absorption via $5d$-$6sp$ transitions leads to photoelectrons with energies <1.1eV above E_F and $5d$ holes at 2 to 3eV below E_F. As radiative decay of $5d$ holes is expected to be insignificant, photo-excitation and Auger decay constitute the primary processes in this early stage. With Auger decay playing a dominant role, what emerges at the end of photo-excitation is a strongly out-of-equilibrium system characterized by a non-Fermi-Dirac electron energy distribution with an excess of $5d$ electrons and a deficit of $6sp$ electrons, accompanied by the presence of energetic photoelectrons and Auger electrons in the $6sp$ band. To reach thermalization, the population of the $5d$ and $6sp$ bands will be regulated by collisional excitation and Auger decay while the $5d$ and $6sp$ electrons relax toward a Fermi-Dirac distribution via electron-electron scattering. As the excitation energy density increases, the lifetime of $5d$ holes appears to be shortened, causing the system to deviates further from equilibrium. More time is then needed for the relaxation of the system. This leads to the increase of electron thermalization time when the excitation energy density is increased, as observed in the experiment.

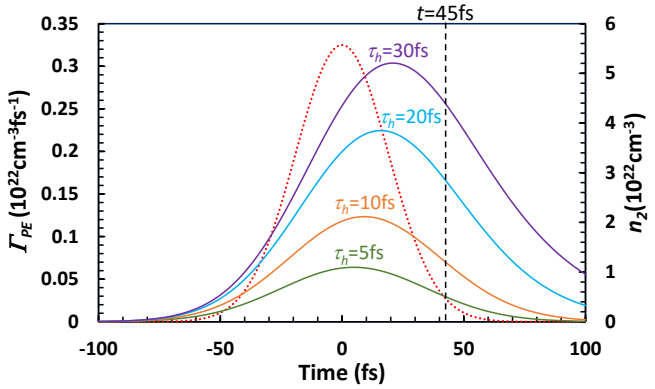

FIG. 5. Plots of (a) $\Gamma_{PE}(t)$ (red dotted line) and (b) $n_2(t)$ that is convoluted with a 51fs(FWHM) Gaussian instrumental function (solid color lines) for excitation energy density of 4MJ/kg.

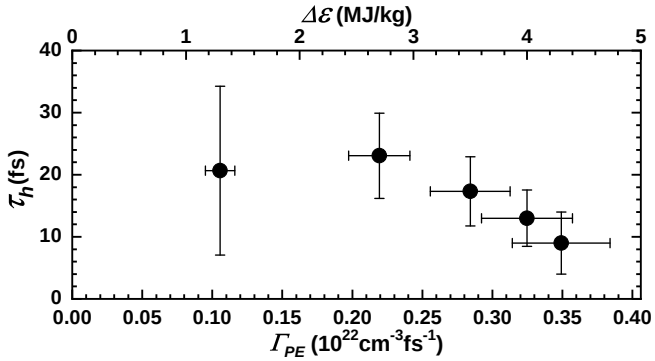

FIG. 6. Lifetime of $5d$ holes as a function of $\Delta\varepsilon$ (top horizontal axis) and Γ_{PE} (bottom horizontal axis).

In conclusion, we have obtained the temporal evolution of ac conductivity and conduction electron density resulting from fs-laser heated Au as the first study of ultrafast photo-excitation of $5d$ electrons at energy densities up to 4.3MJ/kg. The results reveal that (i) photo-excitation is severely mitigated by Auger decay giving rise to a strongly out-of-equilibrium system at the end of the pump laser pulse, (ii) during photo-excitation, the lifetime of $5d$ holes has an upper bound of 10-20fs and decreases with increasing excitation energy density, and (iii) the time for the non-equilibrium electron system to reach thermalization increases from 100fs to 300fs when the excitation energy density is raised from 1.3MJ/kg to 4.3MJ/kg. These findings are unique characteristics for testing non-equilibrium electron kinetics model. They have also been used to construct a physical picture describing the roles of the underlying processes, as guidance for the development of theoretical models.

We thank Advanced Laser Light Source in Canada for technical support and use of facility, and acknowledge the research funding support from Natural Sciences and Engineering Research Council of Canada. Part of this work is performed under the auspices of the U.S. Department of Energy by Lawrence Livermore National Laboratory under Contract DE-AC52-07NA27344.

* zchen2@ualberta.ca
† Current address: SLAC National Accelerator Laboratory, Menlo Park, CA, USA
‡ nga@physics.ubc.ca

[1] K. Widmann, T. Ao, M.E. Foord, D.F. Price, A.D. Ellis, P.T. Springer, and A. Ng, Phys. Rev. Lett. **92**, 125002 (2004).
[2] Z. Chen, B. Holst, S.E. Kirkwood, V. Sametoglu, M. Reid, Y.Y. Tsui, V. Recoules, and A. Ng, Phys. Rev. Lett. **110**, 135001 (2013).
[3] B. Holst, V. Recoules, S. Mazevet, M. Torrent, A. Ng, Z. Chen, S.E. Kirkwoood, V. Sametoglu, and Y.Y. Tsui, Phys. Rev. B **90**, 035121 (2014).
[4] Y. Ping, D. Hanson, I. Koslow, T. Ogitsu, D. Prendergast, E. Schwegler, G. Collins, and A. Ng, Phys. Rev. Lett. **96**, 255003 (2006).
[5] P. Cellier, A. Ng, G. Xu, and A. Forsman, Phys. Rev. Lett. **68**, 2305 (1992).
[6] Th. Lower, V.N. Kondrashov, M. Basko, A. Kendl, J. Meyer-ter-Vehn, R. Sigel and A. Ng, Phys. Rev. Lett. **80**, 400 (1998).
[7] T. Ao, Y. Ping, K. Widmann, D.F. Price, E. Lee, H. Tam, P.T. Springer, and A. Ng, Phys. Rev. Lett. **96**, 055011 (2006).
[8] R. Ernstorfer, M. Harb, C.T. Hebeisen, G. Sciani, T. Dartigalonque, and R.J.D. Miller, Science **323**, 1033 (2009).
[9] B.I. Cho, K. Engelhorm, A.A. Correa, T. Ogitsu, C.P. Weber, H.J. Lee, J. Feng, P.A. Ni, Y. Ping, A.J. Nelson, D. Prendergast, R.W. Lee, R.W. Falcone, and P.A. Heimann, Phys. Rev. Lett. **106**, 167601 (2011).
[10] T.G. White, J. Vorberger, C.R.D. Brown, B.J.B. Crowley, P. Davis, S.H. Glenzer, J.W.O. Harris, D.C. Hochhaus, S. LePape, T. Ma, C.D. Murphy, P. Neumayer, L.K. Pattison, S. Richardson, D.O. Gericke, and G. Gregori, Sci. Reports **2**, 889 (2012).
[11] S.P. Hau-Riege, A. Graf, T. Doppner, R.A. London, J. Krywinski, C. Fortmann, S.H. Glenzer, M. Frank, K. Sokolowski-Tinten, M. Messerschmidt, C. Bostedt, S. Schorb, J.A. Bradley, A. Lutman, D. Rodles, A. Ruedenko, and B. Rudek, Phys. Rev. Lett. **108**, 217402 (2013).
[12] A.L. Daraszewicz, Y. Giret, N. Naruse, Y. Mureooka, J. Yang, D.M. Duffy, A.L. Shluger, and K. Tanimura, Phys. Rev. B **88**, 184101 (2013).
[13] N.J. Hartley, P. Belancourt, D.A. Chapman, T. Doppner, R.P. Drake, D.O. Gericke, S.H. Glenzer, D. Khaghani, S. LePape, T. Ma, P. Neumayer, A. Pak, L. Peters, S. Richardson, J. Vorberger, T.G. White, and G. Gregori, High Energy Density Physics **14**, 1 (2015).
[14] M.Z. Mo, Z. Chen, R.K. Li, M. Dunning, B.B.L. Witte, J.K. Baldwin, L.B. Fletcher, J.B. Kim, A. Ng, R. Redmer, A.H. Reid, P. Shekhar, X.Z. Shen, M. Shen, K. Sokolowski-Tinten, Y.Y. Tsui, Y.Q. Wang, Q. Zheng, X.J. Wang, and S.H. Glenzer Science **360**, 1451 (2018).
[15] Z. Chen, M. Mo, L. Soulard, V. Recoules, P. Hering. Y.Y. Tsui, S.H. Glenzer, and A. Ng Phys. Rev. Lett **121**, 075002 (2018).
[16] W.S. Fann, R. Storz, H.W.K. Tom, and L. Bokor, Phys. Rev. B **46**, 13592 (1992).
[17] A.V. Lugovskoy and I. Bay, Phys. Rev. B **60**, 3279 (1999).
[18] C.K. Sun, F. Vallee, L.H. Acioli, E.P. Ippen, and J.G. Fujimoto, Phys. Rev. B **50**, 15337 (1994).
[19] B.Y. Mueller and B. Rethfeld, Phys. Rev. B **87**, 035139 (2013).
[20] W. Schafer and M. Wegener, *Semiconductor Optics and Transport Phenomena* (Springer-Verlag, Berlin 2002).
[21] H. Haug and A-P Jauho, *Quantum Kinetics in Transport and Optics of Semiconductors* (Springer-Verlag, Berlin 2008).
[22] F. Rossi and T. Kuhn, Rev. Mod. Phys. **74**, 895 (2002).
[23] C.A. Popovici, R.A. Ganeev, F. Vidal, and T. Ozaki, Advanced Laser Light Source Annual Report 2007-2008, 48 (2008)(`lmn.emt.inrs.ca/EN/ALLS_Pub.htm`).
[24] P.B. Johnson and R.W. Christy, Phys. Rev. B **6**, 4370 (1972).
[25] Z. Chen, V. Sametoglu, Y.Y. Tsui, T. Ao, and A. Ng, Phys. Rev. Lett. **108**, 165001 (2012).
[26] A. Forsman, A. Ng, G. Chiu, and R.M. More, Phys. Rev. E **58**, R1248 (1998).
[27] A. Ng, P. Sterne, S. Hansen, V. Recoules, Z. Chen, Y.Y. Tsui, and B. Wilson, Phys. Rev. E **94**, 033213 (2016).
[28] V.P. Zhukov, E.V. Chulkov, and P.M. Echenique, Phys. Rev. B **68**, 045102 (2003).